

FtsZ at mid-cell is essential in *Escherichia coli* until the late stage of constriction

Lauren C. Corbin Goodman¹ and Harold P. Erickson^{1,2,*}

Abstract

There has been recent debate as to the source of constriction force during cell division. FtsZ can generate a constriction force on tubular membranes *in vitro*, suggesting it may generate the constriction force *in vivo*. However, another study showed that mutants of FtsZ did not affect the rate of constriction, whereas mutants of the PG assembly did, suggesting that PG assembly may push the constriction from the outside. Supporting this model, two groups found that cells that have initiated constriction can complete septation while the Z ring is poisoned with the FtsZ targeting antibiotic PC190723. PC19 arrests treadmilling but leaves FtsZ in place. We sought to determine if a fully assembled Z ring is necessary during constriction. To do this, we used a temperature-sensitive FtsZ mutant, FtsZ84. FtsZ84 supports cell division at 30 °C, but it disassembles from the Z ring within 1 min upon a temperature jump to 42 °C. Following the temperature jump we found that cells in early constriction stop constricting. Cells that had progressed to the later stage of division finished constriction without a Z ring. These results show that in *Escherichia coli*, an assembled Z ring is essential for constriction except in the final stage, contradicting the simplest interpretation of previous studies using PC19.

INTRODUCTION

The protein FtsZ is essential to bacterial cytokinesis. Along with its membrane anchor, FtsA, it assembles a Z ring early in the cell cycle. The Z ring subsequently recruits downstream proteins that remodel the peptidoglycan (PG) wall, suggesting that it serves as a scaffold for this recruitment.

An ongoing controversy is what generates the force for constriction. In 2008, Erickson and Osawa found that Z rings containing only membrane-tethered FtsZ could constrict multilayer tubular liposomes [1]. In the presence of FtsA, rings were able to complete constriction [2]. This established the Z ring as a likely source of constriction force. The mechanism of force generation was suggested to be a transition of FtsZ protofilaments from straight to curved, generating a bending force that pulls the cell membrane inward [3].

The Z-centric constriction model was questioned recently when Coltharp and colleagues found that the rate of constriction was not altered by a mutation of FtsZ, but was slowed by a mutation of FtsI, a key component of the PG synthesis machinery [4]. They suggested that the constriction force was generated by FtsI remodelling the PG, pushing the cell membrane from the outside. Erickson and Osawa suggested an alternative explanation, that FtsZ was providing the constriction force, but the rate of constriction was limited by PG remodelling serving as a strong brake [5, 6]. However, the idea of constriction force generated by PG remodelling, with FtsZ serving primarily as a scaffold, has risen to prominence in the field.

More recently, two groups reported that constriction could continue after poisoning the Z ring with the drug PC190723 (abbreviated here as PC19). PC19 is a candidate antibiotic that targets FtsZ [7]. It causes subunits to lock into the T conformation [8]. The T conformation is favoured by assembly into protofilaments, and it produces a high affinity longitudinal bond [9]. PC19 binds to T subunits in the protofilament, preventing the subunits from changing to the weaker R conformation and disassembling. Because of this, PC19 stabilizes protofilaments *in vitro* and presumably *in vivo* [10]. When *Bacillus subtilis* cells were treated with PC19, patches of FtsZ that were treadmilling around the Z ring immediately arrested their movement [11].

Received 25 February 2022; Accepted 06 May 2022; Published 09 June 2022

Author affiliations: ¹Department of Biomedical Engineering, Duke University, Durham, North Carolina, USA; ²Department of Cell Biology, Duke University, Durham, North Carolina, USA.

***Correspondence:** Harold P. Erickson, h.erickson@cellbio.duke.edu

Keywords: FtsZ; divisome; gram-negative; *E. coli*.

Abbreviations: LB, luria broth; Min, minute; PBS, phosphate-buffered saline; PC19, PC190723; PG, peptidoglycan; T jump, temperature jump.

Experiments with PC19 in *Staphylococcus aureus* [12] and *B. subtilis* [13] showed that if the Z ring were poisoned before constriction began, PC19 blocked constriction. However, once constriction had been initiated, it would continue to complete septation in the presence of PC19. This suggested that FtsZ treadmilling is essential for condensation and maturation of the Z ring, but is not essential for constriction. If treadmilling is not essential for constriction, perhaps FtsZ itself is dispensable once constriction has initiated.

A problem with this more global conclusion, that FtsZ may be dispensable for constriction, is that PC19 does not immediately disassemble the Z ring. PC19 and the related benzamide 8j eventually leads to disassembly of FtsZ from the Z ring and redistribution into foci scattered around the cell. However, FtsZ remains at the Z ring for 10–30 min [14].

Could the static, non-treadmilling Z ring still contribute to constriction? Importantly, FtsZ can still form both straight and curved protofilaments in the presence of PC19 [10] and 8j [14]. Thus, while PC19 rapidly arrests treadmilling, it leaves FtsZ in place and potentially able to continue generating a bending force on the membrane. This FtsZ-based force may be essential for the continued constriction after poisoning by PC19.

We sought to determine if an assembled Z ring is necessary during constriction. For this, we employed an FtsZ84 genomic mutant strain of *Escherichia coli*, JFL101, as a tool. JFL101 achieves largely normal division at 30 °C, although the FtsZ84 treadmills more slowly and the cell cycle is longer [15]. At 42 °C, the Z ring disassembles within 1 min [16]. We used a rapid temperature jump (*T* jump) to disassemble the Z ring and observe how the cells respond to the sudden depletion of FtsZ from the Z ring.

METHODS

Cell cultures

All liquid cultures were grown in LB (1% tryptone, 0.5% sodium chloride, 5% yeast extract, 0.2% glucose, pH 7.0) Liquid cultures were started from –20 °C freezer stock (10% glycerol) or streaked plates. We did not find a difference between the methods. We grew liquid cultures in LB at 30 °C overnight. Cultures were spun down and diluted by 200- to 1000-fold into fresh LB and grown for several hours until mid-log phase (OD600 between 0.15 and 0.5) for experiments.

Aliquots of 4% formaldehyde in PBS were prepared less than 1 month ahead of experiment. PBS was heated to 60 °C, and powdered paraformaldehyde was added to a final concentration of 4%. Sodium hydroxide was titrated into the solution until the paraformaldehyde had dissolved. The solution was cooled, and the pH was adjusted to 7.0. The solution was filtered with a 0.22 µm polyethersulfone membrane filter, and aliquots were frozen at –20 °C.

Cell counting

T-jump experiments were performed in a 37 °C incubator room to reduce heat fluctuations while samples were removed and fixed. An Erlenmeyer flask with 50 ml of filtered LB was preheated to 42 °C in a water bath for at least 2 h prior to the start of the experiment. Pipettes, pipette tips, and 2× fixation solutions were also pre-warmed. Formaldehyde was diluted with PBS to produce 2% formaldehyde (2× fixative). The 2× fixative was filtered again within an hour of the start of the *T*-jump experiment. We pre-aliquoted 500 µl of 2× formaldehyde for each sample.

At the start of the *T*-jump experiment, mid-log cells were pre-diluted if needed into fresh 30 °C LB to obtain an OD600 of 0.15. 1.5 ml of cells were added to the 50 ml 42 °C LB. Immediately, 500 µl of cells were removed and diluted into 500 µl 2× fixative, for a final concentration of 1% formaldehyde. We consider this time=0 min. Initially, the temperature of the LB dropped 0.3 °C below 42 °C, but the water bath warmed the LB to 42 °C within a min. We performed this twofold dilution from the 42 °C LB to the 2× fixation at each time point. We also recorded the LB temperature at these time points. We repeated the dilution between 3 and 5 times for each experiment at each time to check for preciseness of the single experiment. We repeated this experiment to obtain four replicates with our desired experimental conditions. Fixed samples were cooled to room temperature and counted within 3 h.

To count the cells, we used the BD FACSCanto II flow cytometry system at medium flow rate. We counted cells for 2 min gated against forward scatter area and side scatter area. We collected blank measurements for each experiment by counting a solution of 500 µl fresh LB plus 500 µl 2× fixative.

We gated and counted the cells in each sample with the free and open source Python package FlowCytometryTools [17, 18]. We highly recommend this package, as it is fast with large FCS files, includes excellent documentation, and is intuitive. We performed data analysis and made figures in R with packages in the Tidyverse [19, 20].

We optimized cell concentration by performing a serial dilution and counting cells. To do this, we serially diluted the fixed cells twofold in filtered PBS. We counted cells for 1 min and plotted the cell count against the calculated cell concentration based on an ideal serial dilution.

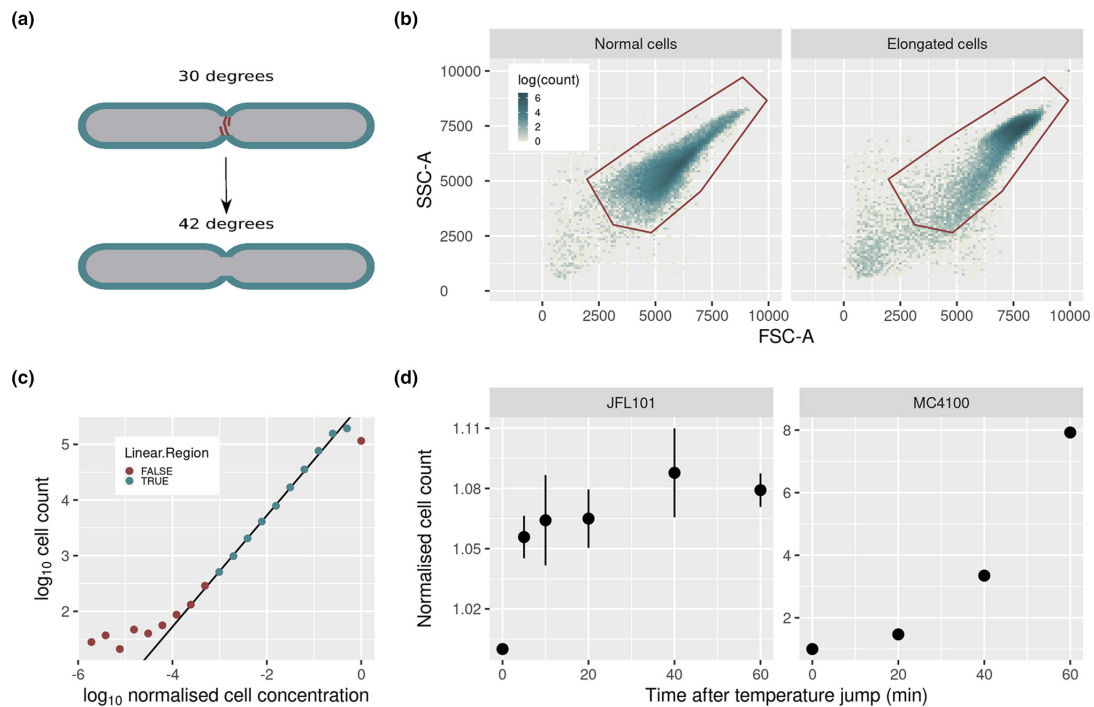


Fig. 1. (a) Diagram of *T*-jump experiment. (b) Representative flow cytometry histograms of normal (left side) and elongated (right side) cells. Red polygons outline the signals counted as cells. SSC-A and FSC-A are log transformed side and forward scatter area. Normal cells were collected immediately after *T* jump. Elongated cells were collected 1 h after *T* jump. (c) Calibrating the valid range of cell counts from a twofold serial dilution of cells. Line represents a linear regression fit where slope=1 and $r^2=0.996$. (d) Mean of normalized cell count over time after *T* jump of JFL101 cells (left side, $n=4$) or MC4100 cells (right, $n=2$). Note the very different y-axis scales. Cell counts for each replicate were normalized to the count at 0 min. Error bars are standard error for left panel; right panel shows average of the duplicate points.

Fixed membrane imaging

Fixative with 4% formaldehyde was thawed from freezer aliquots, and glutaraldehyde from frozen a 25% stock was added to a concentration of 0.4%. The fixative was filtered approximately 1 h prior to the *T* jump. We pre-measured 6 ml aliquots of 4× fixative and warmed it in the 37°C incubator room. We filtered and pre-warmed 100 ml of LB to 42°C.

Cells were grown to mid-log phase as previously described. At the start of the *T*-jump experiment, we diluted 2.5 ml of culture into 100 ml of 42°C LB. To collect a sample, we removed 20 ml of cells and combined it with 6 ml of 4× fixative. After 2 min, we moved the sample to ice. We repeated this for each point in our time series. For the 0 min sample, we diluted 0.5 ml of cells into 20 ml of 30°C LB and added 6 ml of 4× fixative. We stored fixed samples at 4°C overnight.

To image the fixed cells, we pelleted the cells at 4200 g for 5 min and resuspended the cells in 1 ml LB. We pelleted the cells again and resuspended them in 100 μl fresh LB. We added FM4-64 dye (Invitrogen) to a final concentration of 0.7 μg ml⁻¹. We added 25 μl of stained cells to a 2 cm × 6 cm agar pad made with water and 1% agarose. We allowed the sample to dry for 30 min and covered it with a coverslip. We imaged the cells within 3 h of making the pads.

We imaged the cells with STED implemented on a Leica DMI8 microscope. We excited our sample at 516 nm with a white light laser (0.7% of total power) and collected emissions between 615 and 685 nm with a GaAsP HyD detector. We used the 775 nm STED depletion laser at 8% power. We collected a focal series of seven stacks over 1 μm depth. Each pixel measured 21 nm × 21 nm. We performed deconvolution with the Huygens professional software [21].

We segmented the images by hand with LabKit in FIJI [22]. We then analysed the segments in Python3 [18] with our own algorithm that automated the process. For each cell, our script did the following. We used the segmentation data to crop the image to only contain a single cell plus a pad of 2 pixels for each layer in the 3D series. We then obtained the orientation of the cell with SciKit-Image [23] and rotated each cell so the poles are at the top and bottom of the image. For each layer, we determined the perimeter of the cell. To do this, we performed a 2D convolution on each layer with a kernel containing ones measuring 10×5 pixels. We found the top by calculating the centre of mass of the top fifth of the cell with SciPy [24]. Once we found the centre of mass, we stepped down the cell one pixel at a time and determined the left and right sides of the cell by the maximum value of the convolved image. We set conditions that prevented large jumps or boundaries that are not cell width.

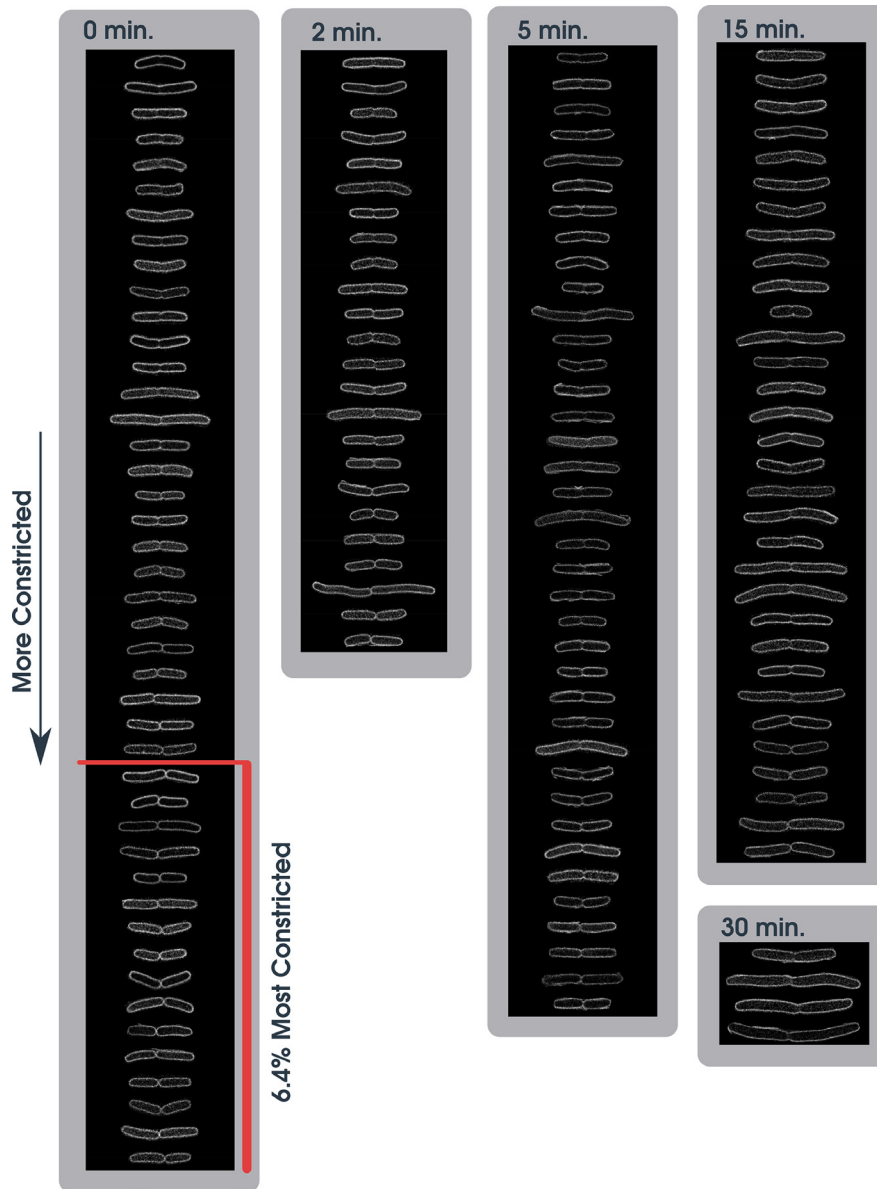


Fig. 2. Cropped images of cells sorted by constriction progress and time point. Cells towards the bottom are the furthest constricted. For time 0 min, the red line denotes the 6.4% most constricted cells (out of total cells). Approximately 80–90% of cells were not constricted and are not shown here.

After we determined the perimeter of the cell, we quantified the cell by first dividing the cell into five parts. We determined the cell width by averaging the width between the left and right boundaries at the top 1/5 and 2/5 and the bottom 3/5 and 4/5. We then measured the widths at the centre fifth of the cell for each row of pixels. If the centre fifth had a width of less than 95% of the cell width, we considered this a constriction. We measured the constriction width as the narrowest two cross-sections in this constriction region. The normalized constriction is the constriction width divided by the cell width.

Live membrane imaging

Cells were grown to mid-log phase as previously described. We pelleted the cells at 1600 g for 5 min and resuspended them in 200 μ l of fresh LB. We added FM5-95 dye (Invitrogen) to a concentration of 4 μ g ml^{-1} from a stock solution in water. We sonicated a glass bottom dish (MatTek) in Helmenex followed by 100% ethanol. We plated 5 μ l of cells onto the glass bottom coverslip dish and covered it with a 1% agarose LB pad, approximately 1–2 cm wide, square. We put a lid on the glass bottom dish and incubated it at 30 $^{\circ}C$ for 30 min.

Table 1. JFL101 cells counted and proportion with constrictions for fixed imaging analysis

Time (min)	Cells counted	Constrictions
0	371	18.1%
2	175	14.9%
5	318	14.5%
15	379	9.0%
30	103	4.9%

To perform the *T* jump, we transferred the glass bottom dish with the cells into a 42.5 °C microscope cage incubator (Oko-lab). We imaged the cells with a Nikon Eclipse Ti2 confocal microscope with NIS Elements software and a heated objective. We excited the sample at 560 nm and collected emissions above 630 nm. We took a time-lapse of a single field of view with one frame/min.

RESULTS

Our experiments all used JFL101 as a tool. JFL101 is a temperature-sensitive FtsZ *E. coli* mutant that behaves similar to wild type at 30 °C (Fig. 1a). However, at 42 °C, the Z ring disassembles within 1 min [16]. For our *T*-jump experiments, we grew JFL101 at 30 °C, and diluted the cells into 42 °C media, causing the Z ring to disassemble. Following this *T* jump we observed the process of septation by several methods.

Counting division by flow cytometry

Our first method characterized the *T* jump using flow cytometry to count cells to determine what fraction of cells could continue constriction to complete division following the sudden depletion of FtsZ from the Z ring. For this we fixed aliquots of cells at set time points following the *T* jump. Before we began this experiment, we optimized flow cytometer settings to ensure we were capturing cells. We were able to isolate the cells by gating against the forward and side scatter area (Fig. 1b, left panel). When JFL101 loses the Z ring, the cells elongate, so we optimized the flow rate, gate and cell density to also capture elongated cells (Fig. 1b, right panel). We found that SYTO BC bacterial stain and propidium iodide stain did not improve our ability to gate the cells.

We first determined the concentration at which we could obtain a valid count of cells. At high concentrations, cells can crowd the central fluid stream and evade being counted. At low concentration, the noise obscures the true count. For calibration, we used a serial dilution assay. After fixing a sample of cells, we serially diluted the cells twofold and counted the cells for 1 min. We found the region in which a twofold dilution would result in a twofold reduction in cell count. This was approximately between 500 and 194000 cells per min (Fig. 1c).

After these optimizations, we then performed the full *T*-jump experiment to disassemble the Z ring, collect fixed samples over time and count the cells. We normalized the cell counting results from each replicate to the replicate's initial average cell count at 0 min. Fig. 1d, left panel, shows the combined results of four replicated *T*-jump experiments. When the JFL101 cells were jumped to 42 °C, the cell count then increased to a plateau at 6.4–6.5% above the zero time at 10 and 20 min. From this, we conclude that 6.4% of cells can complete division without FtsZ assembled in a Z ring.

We repeated this experiment with MC4100, the wild-type *E. coli* strain from which JFL101 was constructed (Fig. 1d, right panel). We found that the *T*-jump treatment did not inhibit division.

Imaging membrane constrictions following the sudden depletion of Z ring

We then wanted to understand what happens to the constricting membrane following the sudden depletion of FtsZ. We repeated the *T*-jump experiment, and imaged the cells after staining the outer membrane with the fluorescent dye FM4-64 [25]. We used the super-resolution technique STED for imaging. We collected images of more than 100 fixed cells at each time point and quantified the extent of constriction. These images created a pseudo-time lapse of constrictions after the *T* jump.

Fig. 2 contains cropped images of cells sorted by their constriction progress and time. Our 0 min sample was collected just before the *T* jump. At this time, we found a wide range of constrictions, from almost fully constricted (bottom of montage) to just beginning constriction (top of montage). Overall, 18.1% of cells were constricted at time 0 min, and this decreased to 9.0% at 15 min (Table 1). The percent constricted cells decreased further at 30 min, perhaps due to relaxation of some early constrictions, as noted previously by Addinall *et al.* [16].

When we performed the *T* jump with wild-type MC4100 *E. coli*, we found an initial decrease in constrictions after the first 15 min (Table 2). The population of constricted cells then rebounded to the initial proportion after 30 min.

Table 2. MC4100 cells counted and proportion with constrictions for fixed imaging analysis

Time (min)	Cells counted	Constrictions
0	145	36.6%
15	206	25.5%
30	121	38.8%

We then measured the extent of constriction over time for JFL101 (Fig. 3a). The normalized constriction is the constriction width divided by the average cell width. A normalized constriction near zero means that the cell has almost completed division. A normalized constriction near one means the cell has just begun constriction. The cells had an average width of $0.822 \pm 0.078 \mu\text{m}$. The overall conclusion from Fig. 3(a) is that cells in early constriction are retained at 2, 5 and 15 min after the *T* jump, while late constricting cells disappear. The disappearance of the late constricting cells is consistent with having completed division. To correlate these data with the cell counting, which showed a 6.4% increase in cells following the *T* jump, we show a line in Fig. 3(a) at 0.44 normalized constriction at 0 time. Altogether, 6.4% of cells are below this line and presumably completed division. We found that MC4100 cells retained a similar range of constrictions after the *T* jump (Fig. 3b).

To further inform our analysis of these results, we repeated the *T*-jump experiment by imaging live cells after a *T* jump on a heated microscope stage. We grew live JFL101 stained with FM5-95 on small agar pads. FM5-95 is also an outer membrane dye but was less toxic and had longer lasting fluorescence than FM4-64 in live cells. We transferred the agar pad to a 42.5°C incubator microscope and imaged the cell's response to the *T* jump. We did not find any cells that initiated constriction after the *T* jump. If a cell was previously constricted at the start of the *T* jump, the cell either completed constriction (Fig. 4b) or maintained a constant constriction (Fig. 4a). Some cells that remained constricted appeared to slowly relax over the course of 30 min (Fig. 4c). The live cell imaging was done in the laboratory of Dr Alexandre Bisson, Brandeis University. These images are presented as examples without statistics.

DISCUSSION

Two previous studies used the compound PC19 to poison the Z ring in *S. aureus* [12] and *B. subtilis* [13]. Both studies found that PC19 blocked initiation of new constrictions, but constrictions that had already begun continued to complete septation. Since PC19 rapidly arrests treadmilling, these results suggest that treadmilling is needed for formation and maturation of the Z ring and to initiate constriction, but treadmilling was not needed for constriction itself. Since PC19 leaves FtsZ in the Z ring for 10–30 min [14], it is possible that the static FtsZ was still contributing to constriction.

The temperature-sensitive FtsZ84 provides a way to rapidly and completely remove FtsZ from the divisome. Addinall *et al.* observed that cells retained sharp constrictions 2 min after the *T* jump, and constrictions remained but became more blunt or rounded after 10 min [16]. In contrast, when PC19 poisoned the Z ring in *S. aureus* and *B. subtilis*, all constrictions disappeared as they completed septation [12, 13].

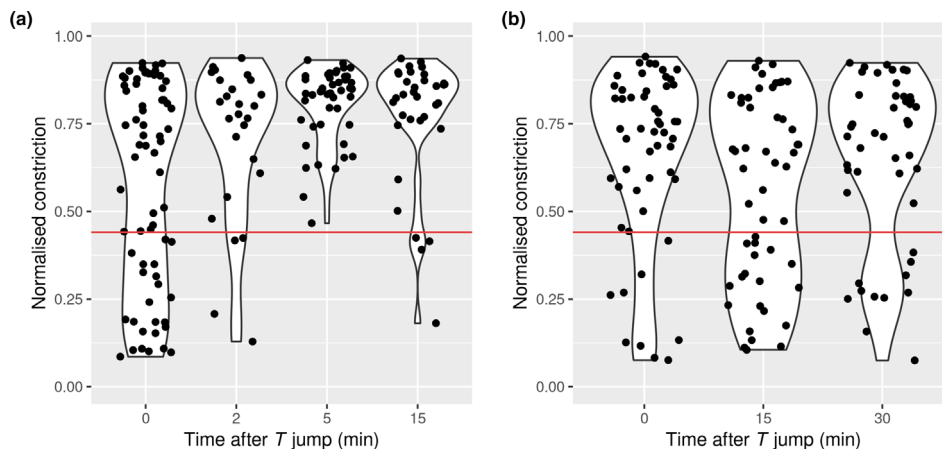


Fig. 3. Density of normalized constriction after *T* jump for JFL101 (a) or MC4100 (b). Unconstricted cells were omitted from these plots, so for 0 min (a), only 18.1% of cells are shown. Red line denotes 6.4% most constricted cells at 0 min relative to the whole population.

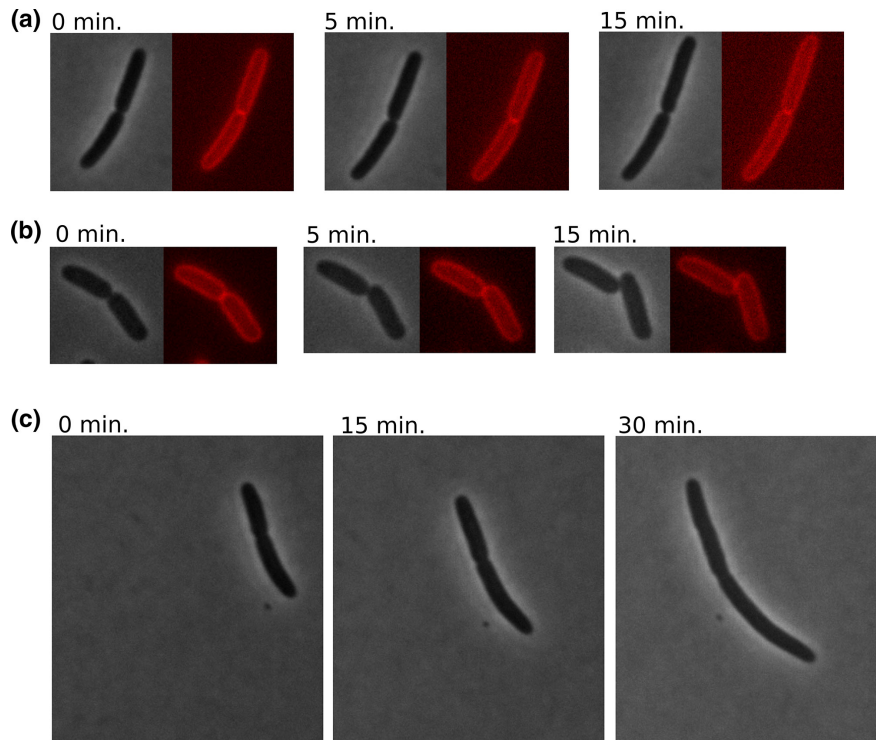


Fig. 4. Live time lapse of JFL101 after *T* jump. Grey panels are phase contrast and red panels are FM5-95 dye. Cells either maintained constriction (a), completed constriction (b), or slowly relaxed (c). In (c) we show only phase contrast because the fluorescence was bleached over 30 min.

As opposed to observations of Addinall *et al.*, our study provides quantitation. Following the *T* jump, we found a 6.4% increase in cell count at 10–20 min (Fig. 1d, left panel). Since 18.1% of cells showed a constriction at 0 min, this suggests that about one third of the constricted cells completed division. Light microscopy showed that cells in late constriction disappeared at 2–15 min, while the fraction of cells in early constriction remained about the same. Apparently cells in early constriction become locked and unable to progress when FtsZ is depleted (Fig. 5). This is in apparent contrast to experiments in *B. subtilis* and *S. aureus*, where both late and early constricted cells progress to complete septation after poisoning with PC19 [12, 13].

That the late constricted cells can complete division without FtsZ is expected from previous studies of Söderström *et al.*, which showed that FtsZ disassembles from the Z ring before constriction is complete [26, 27]. In Söderström *et al.* 2016, the last two frames in their Fig. 5(b) show FtsZ still present at a constriction width of 0.3 μm and gone at a width of 0.2 μm . This shows that cells naturally complete the last $\sim 0.25 \mu\text{m}$ (normalized constriction 0.31) without FtsZ. This is only a single cell, but it is in agreement with more complex numbers based on constriction times normalized to cell-cycle time. Our work suggests that they may be able to complete constriction from a somewhat earlier point if FtsZ is artificially depleted. The 6.4% of cells that can complete division correlates to a normalized constriction of 0.44, or actual width of 0.36 μm (Fig. 3a)

While our experiments expand upon those of Monteiro *et al.* [12] and Whitely *et al.* [13] it is important to note the difference in bacterial species. *S. aureus* and *B. subtilis* are Gram-positive bacteria while our study was of Gram-negative *E. coli*. In

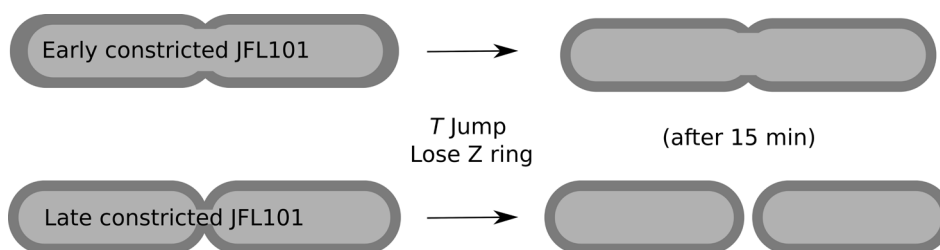


Fig. 5. Diagram of early vs. late cells at zero and 15 min from our experiments.

Gram-positive bacteria, constriction involves a sharp septum at all stages, while Gram-negative bacteria have a shallower V-shaped constriction at earlier stages [28, 29] (but see [5] for a hypothesis uniting the two mechanisms). It will therefore be important to determine if Gram-positive bacteria require FtsZ for early constriction.

Ideally we would like to image downstream proteins, especially FtsI, FtsW and FtsN, to confirm their presence following the depletion of FtsZ. We tried to label FtsI and FtsN separately with mCherry in pRha67 and pJSB2 vectors, however we were unable to obtain reliable fluorescence. It seems likely that FtsI and FtsW remain after FtsZ is depleted in late-constricted cells, since these cells completed division.

A related issue is the two-track model for FtsW proposed by Yang *et al.* [30]. FtsW on one track is moving fast and in concert with FtsZ treadmilling. FtsW on the second track is moving slowly, and movement is dependent on peptidoglycan synthesis. FtsN plays a role in promoting this second track. Since the fast track is correlated with FtsZ treadmilling, it would seem to disappear upon depletion of FtsZ. The slow track involved in peptidoglycan synthesis would seem to remain, since this synthesis should be essential for completing septation.

What generates the force for the late constriction? FtsZ pulling from the inside remains a strong candidate for initiation and early constriction. Our work, and previous studies of Söderström *et al.* [26, 27], show that FtsZ is not needed for late constriction. Here the constriction force may be generated by PG synthesis pushing the membrane from the outside [4]. However, this may require a Brownian ratchet mechanism to move the membrane from contact with PG remodelling enzymes, in order to insert new glycan strands. Such a mechanism has not been developed, and may encounter problems [31].

A third potential force generator is excess membrane production. Once a membrane furrow has been initiated at the division site, excess membrane would push this furrow to continue constriction, rather than initiate new furrows [6]. Evidence for this has come from experiments with L form bacteria, which are bacteria that are modified to survive without their PG cell wall. Leaver and colleagues found that L form *B. subtilis* do not require FtsZ to divide [32]. Instead, it divides with blebs created by excess membrane [33]. That study proposed that excess membrane production may have been the driving force for division of the earliest life form. An *E. coli* L form has been engineered to switch back to the walled state, and it can still divide without FtsZ, although it had switched from the normal cylindrical shape to a branched and bulging, ramified shape, called 'coli-flower' [34]. Excess membrane production could therefore serve as a primary force for late constriction in the normal bacterial cells, with PG synthesis following and filling the gap produced by the advancing membrane.

CONCLUSIONS

In contrast to results of Monteiro *et al.* [12] and Whitley *et al.* [13], where most or all cells that had initiated constriction could complete septation after poisoning with PC19, we found that only cells in late constriction could continue after abrupt depletion of FtsZ. It is important to note two differences in these studies. First, the studies of Monteiro *et al.* [12] and Whitley *et al.* [13] used Gram-positive bacteria, whereas we used Gram-negative *E. coli*. Therefore, the results may be species dependent. Second, our study abruptly depleted FtsZ from the Z ring, where those of Monteiro *et al.* [12] and Whitley *et al.* [13] poisoned treadmilling by PC19, but left FtsZ protofilaments in place. We think the depletion of FtsZ is likely the most important reason that early constriction was arrested in our experiments, but this would need to be addressed by similar experiments in Gram-positive bacteria.

Funding information

The authors received no specific grant from any funding agency.

Conflicts of interest

The authors declare that there are no conflicts of interest.

References

- Osawa M, Anderson DE, Erickson HP. Reconstitution of contractile FtsZ rings in liposomes. *Science* 2008;320:792–794.
- Osawa M, Erickson HP. Liposome division by a simple bacterial division machinery. *Proc Natl Acad Sci U S A* 2013;110:11000–11004.
- Erickson HP, Anderson DE, Osawa M. FtsZ in bacterial cytokinesis: cytoskeleton and force generator all in one. *Microbiol Mol Biol Rev* 2010;74:504–528.
- Coltharp C, Buss J, Plumer TM, Xiao J. Defining the rate-limiting processes of bacterial cytokinesis. *Proc Natl Acad Sci U S A* 2016;113:E1044–53.
- Erickson HP. How bacterial cell division might cheat turgor pressure - a unified mechanism of septal division in Gram-positive and Gram-negative bacteria. *Bioessays* 2017;39:1700045.
- Osawa M, Erickson HP. Turgor pressure and possible constriction mechanisms in bacterial division. *Front Microbiol* 2018;9:111.
- Haydon DJ, Stokes NR, Ure R, Galbraith G, Bennett JM, *et al.* An inhibitor of FtsZ with potent and selective anti-staphylococcal activity. *Science* 2008;321:1673–1675.
- Matsui T, Yamane J, Mogi N, Yamaguchi H, Takemoto H, *et al.* Structural reorganization of the bacterial cell-division protein FtsZ from *Staphylococcus aureus*. *Acta Crystallogr D Biol Crystallogr* 2012;68:1175–1188.
- Corbin LC, Erickson HP. A unified model for treadmilling and nucleation of single-stranded FtsZ protofilaments. *Biophys J* 2020;119:792–805.
- Andreu JM, Schaffner-Barbero C, Huecas S, Alonso D, Lopez-Rodriguez ML, *et al.* The antibacterial cell division inhibitor PC190723 is

- an FtsZ polymer-stabilizing agent that induces filament assembly and condensation. *J Biol Chem* 2010;285:14239–14246.
11. Bisson-Filho AW, Hsu YP, Squyres GR, Kuru E, Wu F, *et al*. Treadmilling by FtsZ filaments drives peptidoglycan synthesis and bacterial cell division. *Science* 2017;355:739–743.
 12. Monteiro JM, Pereira AR, Reichmann NT, Saraiva BM, Fernandes PB, *et al*. Peptidoglycan synthesis drives an FtsZ-treadmilling-independent step of cytokinesis. *Nature* 2018;554:528–532.
 13. Whitley KD, Jukes C, Tregidgo N, Karinou E, Almada P, *et al*. FtsZ treadmilling is essential for Z-ring condensation and septal constriction initiation in *Bacillus subtilis* cell division. *Nat Commun* 2021;12:2448.
 14. Adams DW, Wu LJ, Czaplowski LG, Errington J. Multiple effects of benzamide antibiotics on FtsZ function. *Mol Microbiol* 2011;80:68–84.
 15. Yang X, Lyu Z, Miguel A, McQuillen R, Huang KC, *et al*. GTPase activity-coupled treadmilling of the bacterial tubulin FtsZ organizes septal cell wall synthesis. *Science* 2017;355:744–747.
 16. Addinall SG, Cao C, Lutkenhaus J. Temperature shift experiments with an ftsZ84(Ts) strain reveal rapid dynamics of FtsZ localization and indicate that the Z ring is required throughout septation and cannot reoccupy division sites once constriction has initiated. *J Bacteriol* 1997;179:4277–4284.
 17. Yurtsev E, Friedman J, Gore J. FlowCytometryTools: version 0.4.5. *Zenodo* 2015.
 18. van Rossum G, Drake FL. *Python 3 Reference Manual*. Scotts Valley, CA: CreateSpace; 2009. <https://docs.python.org/3/reference/>
 19. R Core Team. *R: A Language and Environment for Statistical Computing*. Vienna, Austria: R Foundation for Statistical Computing; 2021.
 20. Wickham H, Averick M, Bryan J, Chang W, McGowan L, *et al*. Welcome to the tidyverse. *JOSS* 2019;4:1686.
 21. SV Imaging. Huygens Professional; (n.d.). <https://svi.nl/Huygens-Professional>
 22. Arzt M, Deschamps J, Schmied C, Pietzsch T, Schmidt D, *et al*. LABKIT: Labeling and Segmentation Toolkit for Big Image Data. *Front Comput Sci* 2022;4.
 23. van der Walt S, Schönberger JL, Nunez-Iglesias J, Boulogne F, Warner JD, *et al*. scikit-image: image processing in Python. *PeerJ* 2014;2:e453.
 24. Virtanen P, Gommers R, Oliphant TE, Haberland M, Reddy T, *et al*. Author Correction: SciPy 1.0: fundamental algorithms for scientific computing in Python. *Nat Methods* 2020;17:261–272.
 25. Pilizota T, Shaevitz JW. Plasmolysis and cell shape depend on solute outer-membrane permeability during hyperosmotic shock in *E. coli*. *Biophys J* 2013;104:2733–2742.
 26. Söderström B, Skoog K, Blom H, Weiss DS, von Heijne G, *et al*. Disassembly of the divisome in *Escherichia coli*: evidence that FtsZ dissociates before compartmentalization. *Mol Microbiol* 2014;92:1–9.
 27. Söderström B, Mirzadeh K, Toddo S, von Heijne G, Skoglund U, *et al*. Coordinated disassembly of the divisome complex in *Escherichia coli*. *Mol Microbiol* 2016;101:425–438.
 28. Szwedziak P, Wang Q, Bharat TAM, Tsim M, Löwe J. Architecture of the ring formed by the tubulin homologue FtsZ in bacterial cell division. *Elife* 2014;3:e04601.
 29. Judd EM, Comolli LR, Chen JC, Downing KH, Moerner WE, *et al*. Distinct constrictive processes, separated in time and space, divide *Caulobacter* inner and outer membranes. *J Bacteriol* 2005;187:6874–6882.
 30. Yang X, McQuillen R, Lyu Z, Phillips-Mason P, De La Cruz A, *et al*. A two-track model for the spatiotemporal coordination of bacterial septal cell wall synthesis revealed by single-molecule imaging of FtsW. *Nat Microbiol* 2021;6:584–593.
 31. Pollard TD. Theory from the oster laboratory leaps ahead of experiment in understanding actin-based cellular motility. *Biophys J* 2016;111:1589–1592.
 32. Leaver M, Domínguez-Cuevas P, Coxhead JM, Daniel RA, Errington J. Life without a wall or division machine in *Bacillus subtilis*. *Nature* 2009;457:849–853.
 33. Mercier R, Kawai Y, Errington J. Excess membrane synthesis drives a primitive mode of cell proliferation. *Cell* 2013;152:997–1007.
 34. Mercier R, Kawai Y, Errington J. Wall proficient *E. coli* capable of sustained growth in the absence of the Z-ring division machine. *Nat Microbiol* 2016;1:16091.

Edited by: T. Palmer

Five reasons to publish your next article with a Microbiology Society journal

1. The Microbiology Society is a not-for-profit organization.
2. We offer fast and rigorous peer review – average time to first decision is 4–6 weeks.
3. Our journals have a global readership with subscriptions held in research institutions around the world.
4. 80% of our authors rate our submission process as 'excellent' or 'very good'.
5. Your article will be published on an interactive journal platform with advanced metrics.

Find out more and submit your article at microbiologyresearch.org.